Journal of Cellular Biochemistry 103:413–433 (2008)

ARTICLES

Microarray Analyses of Transdifferentiated Mesenchymal Stem Cells

Tatjana Schilling,[1] Robert Küffner,[2] Ludger Klein-Hitpass,[3] Ralf Zimmer,[2] Franz Jakob,[1] and Norbert Schütze[1]*

[1]University of Würzburg, Orthopedic Department, Orthopedic Center for Musculoskeletal Research, Würzburg, Germany
[2]Ludwig Maximilians University of Munich, Department of Informatics, Bioinformatics, Munich, Germany
[3]University of Duisburg-Essen, Institute of Cell Biology (Tumor Research), Essen, Germany

Abstract The molecular events associated with the age-related gain of fatty tissue in human bone marrow are still largely unknown. Besides enhanced adipogenic differentiation of mesenchymal stem cells (MSCs), transdifferentiation of osteoblast progenitors may contribute to bone-related diseases like osteopenia. Transdifferentiation of MSC-derived osteoblast progenitors into adipocytes and vice versa has previously been proven feasible in our cell culture system. Here, we focus on mRNA species that are regulated during transdifferentiation and represent possible control factors for the initiation of transdifferentiation. Microarray analyses comparing transdifferentiated cells with normally differentiated cells exhibited large numbers of reproducibly regulated genes for both, adipogenic and osteogenic transdifferentiation. To evaluate the relevance of individual genes, we designed a scoring scheme to rank genes according to reproducibility, regulation level, and reciprocity between the different transdifferentiation directions. Thereby, members of several signaling pathways like FGF, IGF, and Wnt signaling showed explicitly differential expression patterns. Additional bioinformatic analysis of microarray analyses allowed us to identify potential key factors associated with transdifferentiation of adipocytes and osteoblasts, respectively. Fibroblast growth factor 1 (FGF1) was scored as one of several lead candidate gene products to modulate the transdifferentiation process and is shown here to exert inhibitory effects on adipogenic commitment and differentiation. J. Cell. Biochem. 103: 413–433, 2008.

Key words: transdifferentiation; mesenchymal stem cells; osteoblast; adipocyte; microarray analysis

Maintenance and regeneration of bone requires the differentiation of human mesenchymal stem cells (hMSCs) into osteoblasts [Krane, 2005; Martin and Sims, 2005]. Besides generation of osteoblasts, the multipotential hMSCs can also generate adipocytes and other mesenchymal cell lineages [Prockop, 1997; Pittenger et al., 1999; Muraglia et al., 2000; Verfaillie, 2002; Nöth et al., 2002a; Barry and Murphy, 2004]. Since adipogenic degeneration in the bone marrow and bone-associated diseases like osteoporosis and osteopenia have been reported to increase with aging, an inverse relationship between osteogenic and adipogenic differentiation of hMSCs has been assumed [Meunier et al., 1971; Burkhardt et al., 1987; Beresford et al., 1992; Koo et al., 1998; Nuttall and Gimble, 2000; Pei and Tontonoz, 2004; Gimble et al., 2006; Rosen and Bouxsein, 2006]. Further evidence for this inverse relationship was obtained in a mouse model, where over-expression of 12/15-lipoxygenase that indirectly stimulates adipogenesis caused osteopenia in these animals [Klein et al., 2004]. Thus, a reduction of the capability of hMSCs to differentiate into osteoblasts thereby favoring adipogenesis as well as transdifferentiation of committed osteoblasts into adipocytes could contribute to the adipogenic degeneration.

This article contains supplementary material, which may be viewed at the Journal of Cellular Biochemistry website at http://www.interscience.wiley.com/jpages/0730-2312/suppmat/index.html.

Grant sponsor: Deutsche Forschungsgemeinschaft; Grant number: SCHU 747/7-1.

*Correspondence to: Norbert Schütze, University of Würzburg, Orthopedic Department, Orthopedic Center for Musculoskeletal Research, Molecular Orthopedics, Brettreichstr. 11, D-97074 Würzburg, Germany.
E-mail: n-schuetze.klh@mail.uni-wuerzburg.de

Received 21 December 2006; Accepted 18 April 2007
DOI 10.1002/jcb.21415

Transdifferentiation occurs when a committed cell type that already develops along a certain differentiation pathway (e.g., a pre-osteoblast) changes into a cell type of another differentiation lineage (e.g., an adipocyte). Such phenotype switches between committed or differentiated osteoblasts and adipocytes have been reported by us and others [Nuttall et al., 1998; Park et al., 1999; Schiller et al., 2001; Schilling et al., 2007], even at the single cell level [Song and Tuan, 2004]. The signaling molecules and pathways leading to adipogenic or osteogenic transdifferentiation are completely unknown. If and to what extent established key factors and signaling pathways of normal osteogenesis and adipogenesis are involved in the reprogramming process is also unknown so far.

Osteogenesis is induced by runt-related transcription factor 2 (RUNX2) and osterix [Ducy et al., 1997; Ducy, 2000; Nakashima et al., 2002; Nakashima and de Crombrugghe, 2003]. It is further enhanced via extracellular signal-regulated kinases 1 and 2 involved in the mitogen-activated protein kinase pathway [Jaiswal et al., 2000; Xiao et al., 2002], by bone morphogenetic protein 2, and Δ FBJ murine osteosarcoma viral oncogene homolog B (Δ FOSB) [Gori et al., 1999; Sabatakos et al., 2000]. Adipogenesis is induced by the sequential action of C/CAAT enhancer binding proteins (CEBPs) and peroxisome proliferator-activated receptor γ 2 (PPARG2) [Tanaka et al., 1997; Darlington et al., 1998; Wu et al., 1999; Rosen et al., 2000] that results in enhanced expression of other adipocyte-specific genes like acetyl CoA carboxylases and fatty acid binding protein 4 (FABP4) [Spiegelman et al., 1993].

Transdifferentiation of hMSC-derived osteoblast progenitors and adipocytes into adipocytes and osteoblasts, respectively, was demonstrated in our previous work [Schilling et al., 2007]. Since the molecular mechanisms provoking this reprogramming are unknown, we analyzed genome-wide gene expression patterns by employment of an Affymetrix GeneChip representing 38,500 genes and by development of a novel scoring scheme that evaluates the relevance of regulated genes in the processes of transdifferentiation. Our findings serve as prerequisite for functional examinations of promising candidates that could be involved in signaling pathways provoking transdifferentiation or even acting as switches between the adipogenic and osteogenic lineage. Thereby, functional examination of fibroblast growth factor 1 (FGF1) as one of the potential key factors was proven to inhibit adipogenic lineage development.

MATERIALS AND METHODS

Chemicals were obtained from Sigma–Aldrich (Munich, Germany) unless specified otherwise. Cell culture media were purchased from PAA (Cölbe, Germany), fetal bovine serum (FBS) from Gibco (Karlsruhe, Germany) or PAA (Cölbe, Germany).

Isolation and Culture Expansion of hMSCs

hMSCs from trabecular bone were isolated from the femoral heads of patients undergoing hip replacement surgery due to age-related or hip dysplasia-related attrition and cultivated as described previously [Haynesworth et al., 1992; Nöth et al., 2002b; Schütze et al., 2005a]. Patients were otherwise healthy and did not receive medications with relation to bone metabolism. Experiments were performed upon approval by the Local Ethics Committee of the University of Würzburg and informed consent from each patient (seven female patients aged 40–75 years and one male patient aged 49 years). Cells were propagated in expansion medium consisting of DMEM/Ham's F-12 (1:1) with L-glutamine supplemented with 10% heat inactivated FBS, 1 U/ml penicillin, 100 μg/ml streptomycin (PAA), and 50 μg/ml L-ascorbic acid 2-phosphate. Cells were plated for (trans-) differentiation experiments in passage 1 or 2.

Differentiation and Transdifferentiation of hMSCs

Differentiation and transdifferentiation of hMSCs were performed as described previously [Schilling et al., 2007]. Briefly, osteogenic differentiation of hMSCs was achieved by incubation of confluent hMSC monolayers in osteogenic medium (OM) consisting of expansion medium additionally supplemented with 10 mM β-glycerophosphate and 100 nM dexamethasone for up to 4 weeks [Jaiswal et al., 1997; Schütze et al., 2005b]. Confluent hMSCs formed adipocytes after exposure to adipogenic medium (AM) consisting of DMEM high glucose with L-glutamine supplemented with 10% heat-inactivated FBS, 1 U/ml penicillin, 100 μg/ml streptomycin, 1 μM dexamethasone, 100 μM indomethacin, 500 μM 3-isobutyl-1-methyl-

xanthine, and 1 μg/ml insulin after 2 weeks [Pittenger et al., 1999; Schütze et al., 2005b].

Transdifferentiation of committed osteoblasts (14 days in OM) was performed by subsequent incubation in AM for another 14 days. Analogously, fully differentiated adipocytes (14 days in AM) were transdifferentiated into osteoblasts by exposure to OM for another 4 weeks.

Confluent hMSCs, plated at a density of 7.5×10^4 cells per well onto 4 well-Lab-Tek Chamber Slides (Nunc, Wiesbaden, Germany), received 20 U/ml heparin sodium salt [Wesche et al., 2005] plus 6, 12, or 25 ng/ml recombinant human FGF1 (R&D Systems, Wiesbaden-Nordenstadt, Germany) during incubation in AM for up to 14 days. FGF1 was dissolved in sterile PBS (Biochrom, Berlin, Germany) containing 0.1% bovine serum albumin. Adipogenic lineage development was visualized in undifferentiated monolayers and after 7 and 14 days of incubation in AM with or without FGF1 by staining of intracellular lipid vesicles as described by Pittenger et al. [1999] using Oil Red O (Merck, Darmstadt, Germany) and hemalaun as counterstain for cell nuclei. The amount of lipid vesicle accumulation was semiquantitatively determined for 3 and 4 independent experiments after 7 and 14 days of incubation, respectively. Thereby, six randomly taken microphotographs of each incubation condition were analyzed for the size of lipid vesicle-containing areas per field using Adobe Photoshop CS 8.0.1. Significance of changes was examined by Mann–Whitney U test.

Isolation of RNA

Total RNA was isolated using Trizol Reagent (Invitrogen, Karlsruhe, Germany) and RNeasy Mini Kit (Qiagen, Hilden, Germany) according to the manufacturer's instructions. RNA was obtained from transdifferentiated cells 3 and 24 h after changing to the respective other differentiation medium (i.e., 3 and 24 h after initiation of transdifferentiation) as well as from (pre)differentiated cells 3 and 24 h after renewal of the same kind of differentiation medium (differentiated controls).

Genome-Wide Gene Expression Profiling

Genome-wide gene expression profiling was performed using Affymetrix GeneChips HG-U 133 Plus 2.0 (High Wycombe, United Kingdom) and kits according to the Affymetrix GeneChip Expression Analysis Technical Manual (www.affymetrix.com). In short, biotinylated cRNA samples were prepared from total RNA samples and hybridized onto GeneChips containing probe sets for 47,400 transcripts and 38,500 genes, respectively (http://www.affymetrix.com/support/technical/datasheets/human_datasheet.pdf). Hybridization signals detected with the Affymetrix GeneChip Scanner 3000 were analyzed by Affymetrix GeneChip Operating Software 1.2 and Data Mining Tool 3.1. The expression profiles of transdifferentiated cells were compared to those of (pre)differentiated controls 3 and 24 h after initiation of transdifferentiation, respectively. Differential expression was stated, if a distinct transcript met the following criteria: Increase or decrease call corresponding to a change P-value <0.001 or >0.999 in at least one of the two compared signals, signal $\log_2$ ratio ≤ -1 or ≥ 1 (representing a fold change of at least 2), and present call in at least one of the two compared samples. Each microarray experiment was performed twice with RNA samples from different MSC charges. Altogether, 16 GeneChips were used to examine the two transdifferentiation directions in biological duplicates assessing two time points per transdifferentiation direction.

Further information on gene products was obtained from the NetAffx analysis center (http://www.affymetrix.com), the Invitrogen iPath tool (http://www.invitrogen.com) or from http://www.genecards.org. For GOstat analyses of differentially regulated gene products, the software at http://gostat.wehi.edu.au [Beissbarth and Speed, 2004] was used employing the Benjamini and Hochberg [1995] correction. All Affymetrix IDs on the applied GeneChip that showed at least one P detection call in the two compared samples in each of the duplicated experimental sets served as reference.

Ranking of Differentially Expressed Genes

A novel, empirical scoring scheme has been developed to prioritize genes for further analyses. It was designed to award high scores to significantly regulated genes if their regulation is reciprocal between the two transdifferentiation pathways. The score also assesses the reproducibility of regulation events across datasets from different biological samples.

We took only probe sets into account if an Increase or Decrease call had been attributed by the Affymetrix comparison algorithm. The

extent of regulation was determined via log fold changes between corresponding pairs of transdifferentiation signal versus control intensities. The reliability of the underlying intensity estimates has been factored in by weighting the log fold changes by log change *P*-values. The weighted fold changes exhibited a unimodal, almost symmetrical distribution. We used z-scores of the weighted fold changes to empirically quantify the strength of regulation given the intensity distribution of individual arrays. z-scores for the individual time points have been combined to select probe sets with high fold changes, preferably reciprocal between different transdifferentiation directions. Here, AC:OB indicates osteogenic and OB:AC adipogenic transdifferentiation. The third component evaluates if the intensity difference between 3 and 24 h is also reciprocal. The score_S quantifies reciprocal regulation for probe set s from RNA sample r:

$$\begin{aligned}\text{score}_S(s, r) = &\left|z_{3\,h}^{AC:OB}(s, r) - z_{3\,h}^{OB:AC}(s, r)\right| \\ &+ \left|z_{24\,h}^{AC:OB}(s, r) - z_{24\,h}^{OB:AC}(s, r)\right| \\ &+ \left|z_{24-3\,h}^{AC:OB}(s, r) - z_{24-3\,h}^{OB:AC}(s, r)\right|\end{aligned}$$

Gene scores were computed from the set of probe sets $g_{s,r}$ that measure gene g in sample r:

$$\text{score}_G(g, r) = \frac{1}{\sqrt{|g_{s,r}|}} \sum_{s \in g_{s,r}} \text{score}_S(s, r)$$

The gene scores derived from single RNA samples $r \in R$ were averaged over the set of samples R. This average was weighted with an uncentered correlation coefficient to award higher scores if time courses in R are reproducible. Genes were thus ranked for relevance via:

$$\begin{aligned}\text{score}_{G,R}(g) = &\ \text{ucorr}(z(r_1), z(r_2)) \\ &\cdot \frac{1}{|R|} \sum_{r \in R} \text{score}_G(g, r), \text{ with}\end{aligned}$$

$$\begin{aligned}z(r) = \mathop{++}_{s \in g_{s,r}} \Big\langle &z_{3\,h}^{AC:OB}(s, r) - z_{3\,h}^{OB:AC}(s, r), \\ &z_{24\,h}^{AC:OB}(s, r) - z_{24\,h}^{OB:AC}(s, r), \\ &z_{24-3\,h}^{AC:OB}(s, r) - z_{24-3\,h}^{OB:AC}(s, r)\Big\rangle\end{aligned}$$

Thereby, the individual scores, that is, $\text{score}_G(g,r)$ (score 1 and 2 in Table IV), rank a gene g based on the first and the second measured sample r, whereas the combined score, that is, $\text{score}_{G,R}(g)$, assesses the total relevance of the gene.

Semiquantitative Reverse Transcriptase Polymerase Chain Reaction (RT-PCR)

One microgram total RNA was used to synthesize cDNA by BioScript reverse transcriptase (Bioline, Luckenwalde, Germany) and random hexamers (Amersham, Munich, Germany) according to the manufacturer's instructions. PCR reactions were run in a PTC-200 Peltier thermal cycler (Biozym, Hessisch Oldendorf, Germany) in a volume of 30 μl as described previously [Schütze et al., 2005b] applying 23–40 amplification cycles. For each sample, the PCR reaction mix consisted of 0.5 units BIOTAQ DNA polymerase, 1× NH_4 reaction buffer with 1.7 mM $MgCl_2$, 0.3 mM dNTPs (all Bioline, Luckenwalde, Germany), 5 pmol forward and 5 pmol reverse primer (Operon, Köln, Germany; or Biomers.net, Ulm, Germany) plus 1 μl cDNA. Oligo-nucleotide sequences were chosen by employing free software at http://frodo.wi.mit.edu/cgi-bin/primer3/primer3_www.cgi created by the Whitehead Institute for Biomedical Research [Rozen and Skaletsky, 2000] (Table I). The specificity of PCR products was affirmed by sequencing analyses using the Big Dye Terminator v1.1 Cycle Sequencing Kit and ABI PRISM 310 Genetic Analyzer (Applied Biosystems, Darmstadt, Germany) according to the manufacturer's instructions.

Transcript amounts were evaluated by gel electrophoresis and densitometric analysis as described previously [Schütze et al., 2005b] using the LTF Bio 1D software (LTF, Wasserburg, Germany). Thereby, mRNA amounts were normalized on EEF1A1 mRNA amounts serving as internal control.

RESULTS

Genome-Wide Gene Expression Analysis During Transdifferentiation

We recently showed that hMSCs derived from trabecular bone not only differentiated into osteoblasts and adipocytes, respectively, but also already committed or even differentiated cells derived from these adult hMSCs still gave rise to the other differentiated phenotype, that is, transdifferentiated, when the respective differentiation medium was changed [Schilling

TABLE I. Primer Sequences and Conditions of RT-PCR

Gene name	Primer sequences	Annealing temperature	Accession number
Cysteine-rich angiogenic inducer 61 (CYR61)	Forward: 5′-CAACCCTTTACAAGGCCAGA-3′ Reverse: 5′-TGGTCTTGCTGCATTTCTTG-3′	55°C	NM_001554
Eukaryotic translation elongation factor 1 alpha 1 (EEF1A1)	Forward: 5′-AGGTGATTATCCTGAACCATCC-3′ Reverse: 5′-AAAGGTGGATAGTCTGAGAAGC-3′	54°C	NM_001402
Fatty acid binding protein 4, adipocyte (FABP4)	Forward: 5′-AACCTTAGATGGGGGTGTCC-3′ Reverse: 5′-ATGCGAACTTCAGTCCAGGT-3′	57°C	NM_001442
Fibroblast growth factor 1 (FGF1)	Forward: 5′-CACAGTGGATGGGACAAGG-3′ Reverse: 5′-CTTGAGGCCAACAAACCAAT-3′	54°C	NM_000800 NM_033136 NM_033137
G0/G1switch 2 (G0S2)	Forward: 5′-CGTGCCACTAAGGTCATTCC-3′ Reverse: 5′-TGCACACAGTCTCCATCAGG-3′	57°C	NM_015714
Insulin-like growth factor 1 (somatomedin C) (IGF1)	Forward: 5′-TGGATGCTCTTCAGTTCGTG-3′ Reverse: 5′-CTGACTTGGCAGGCTTGAG-3′	55°C	NM_000618
Kruppel-like factor 6 (KLF6)	Forward: 5′-CTCATGGGAAGGGTGTGAGT-3′ Reverse: 5′-CAGGATCCACCTCTCTGCTC-3′	55°C	NM_001300
Nuclear receptor subfamily 4, group A, member 2 (NR4A2)	Forward: 5′-TTTCTGCCTTCTCCTGCATT-3′ Reverse: 5′-TGTGTGCAAAGGGTACGAAG-3′	57°C	NM_006186 NM_173171 NM_173172 NM_173173
Regulator of G-protein signaling 4 (RGS4)	Forward: 5′-AGTCCCAAGGCCAAAAAGAT-3′ Reverse: 5′-ACGGGTTGACCAAATCAAGA-3′	55°C	NM_005613
Secreted frizzled-related protein 2 (SFRP2)	Forward: 5′-AAAGGTATGTGAAGCCTGCAA-3′ Reverse: 5′-TTGCTCTTGGTCTCCAGGAT-3′	54°C	NM_003013
Serpin peptidase inhibitor, clade E (nexin, plasminogen activator inhibitor type 1), member 1 (SERPINE1)	Forward: 5′-CCGAGGAGATCATCATGGAC-3′ Reverse: 5′-GGAGTTTCTTCTTTCCCGATG-3′	57°C	NM_000602
Tumor necrosis factor receptor superfamily, member 11b (osteoprotegerin) (TNFRSF11B)	Forward: 5′-TAAAACGGCAACACAGCTCA-3′ Reverse: 5′-GCCTCAAGTGCCTGAGAAAC-3′	55°C	NM_002546

et al., 2007]. Osteogenic differentiation into committed pre-osteoblasts was detectable after 14 days in osteogenic medium by expression of osteoblast-specific alkaline phosphatase (ALP) and bone gamma-carboxyglutamate (gla) protein (osteocalcin) (BGLAP) mRNAs as well as homogenous staining for ALP activity all over the monolayers. Differentiation of hMSCs as well as transdifferentiation of mature adipocytes into fully differentiated osteoblasts was obtained after 28 days of incubation in osteogenic medium showing expression of the osteogenic mRNA markers as well as staining for mineralized extracellular matrix. Since besides the osteogenic markers low expression of adipogenic marker mRNAs (PPARG2 and lipoprotein lipase (LPL)) was detected after 28 days of incubation of hMSCs in osteogenic medium, committed osteoblasts obtained after 14 days of osteogenic incubation already expressing specific markers but no adipogenic ones were chosen for adipogenic transdifferentiation. Differentiation of hMSCs as well as transdifferentiation of the committed osteoblasts into mature adipocytes was achieved after 14 days of incubation in adipogenic medium as monitored by formation of homogeneous lipid vesicle accumulation and high expression levels of the adipogenic marker mRNAs. In our previous work, gene expression changes after the initiation of adipogenic transdifferentiation were examined for a single MSC charge by employing the small Affymetrix GeneChip HG-U 133A that was able to detect the expression of 14,500 genes. In the present study, we analyzed the genome-wide expression patterns of both, the adipogenic and the osteogenic transdifferentiation by employing the Affymetrix GeneChip HG-U 133 Plus 2.0 that is able to detect the regulation of 38,500 different human genes. Furthermore, two biological replicates were assessed for each transdifferentiation direction. Each experiment examined the differential mRNA amounts of the genes by comparing RNA samples from transdifferentiated cells with those of normally differentiated cells 3 and 24 h after initiation of transdifferentiation, respectively (Fig. 1).

The analyses yielded 414 and 922 reproducibly regulated genes for adipogenic and osteogenic transdifferentiation, respectively. Genes were regulated at one or both time points

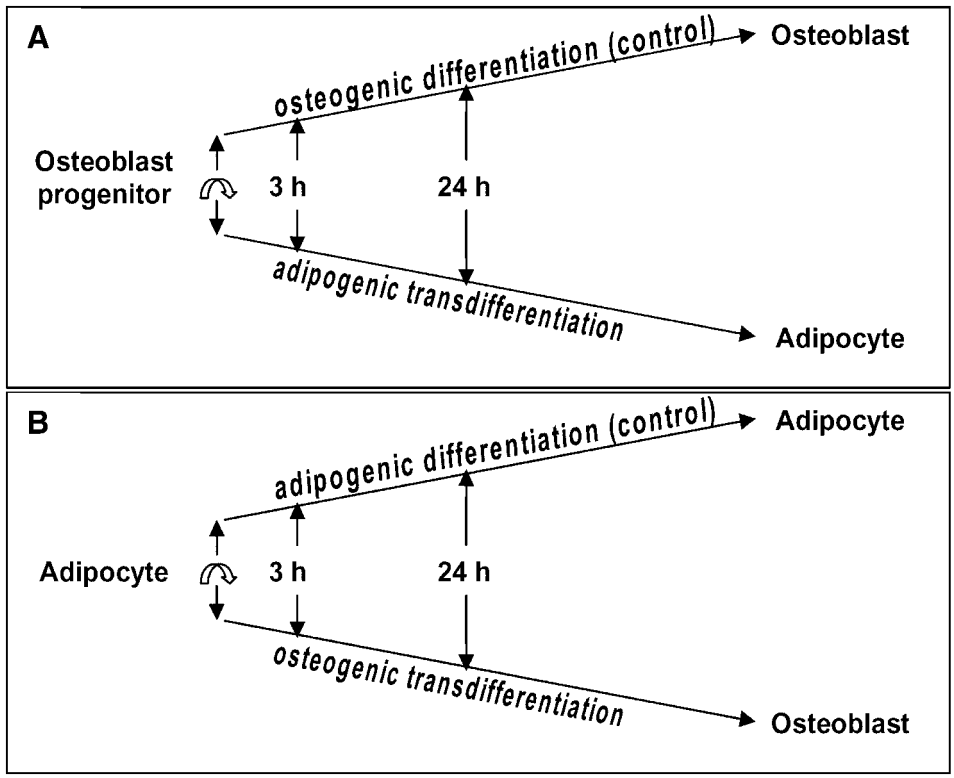

Fig. 1. Schematic illustration of incubation conditions and RNA isolation time points during (trans)differentiation. **A**: Starting from osteoblast progenitors (derived from hMSCs incubated for 14 days in osteogenic medium (OM)), control samples were further incubated in fresh OM whereas transdifferentiated samples were obtained by changing from OM to adipogenic medium (AM) at the same time point (bent arrow). **B**: Adipocytes (derived from hMSCs incubated for 14 days in AM) were further held in fresh AM to obtain control samples, osteogenic transdifferentiation of these adipocytes was achieved by changing from AM to OM at the same time point (bent arrow). For both transdifferentiation directions, RNA samples from transdifferentiated cells isolated 3 and 24 h after initiation of transdifferentiation were compared to RNA control samples isolated after the same time periods but incubated in the same differentiation medium as applied before.

examined (Fig. 2). In particular, switching from committed osteoblasts into differentiated adipocytes revealed regulation of 118 and 324 genes 3 and 24 h after changing the medium, respectively. Thereof, the mRNA levels of 246 genes were decreased whereas those of 168 genes were elevated. The switch from adipocytes into osteoblasts was accompanied by regulation of 76 and 881 genes 3 and 24 h after initiation of transdifferentiation, respectively. Here, mRNA levels of 359 genes were reduced and those of 563 genes were increased. Regulated transcripts are completely listed online (supplementary Tables I–IV).

GOstat analyses of regulated gene products provided over-represented GO classes, a selection of which is stated in Table II (complete results in supplementary Table V). Throughout both transdifferentiation processes, enrichment of gene products associated with the major GO classes of development, transcription, signal transduction, extracellular region, and cytoskeleton was obtained.

Confirmation of Microarray Data by Semiquantitative RT-PCR

The mRNA levels of 11 differentially regulated genes with at least twofold regulation (Table I) were assessed by semiquantitative RT-PCR analysis using the same RNA samples as for the second microarray set of adipogenic and osteogenic transdifferentiation (Fig. 3). Each time point of RNA isolation in each transdifferentiation direction was considered as a single process (Table III). The selected 11 genes provided 28 transdifferentiation processes of which 23 were confirmed, that is, regulation

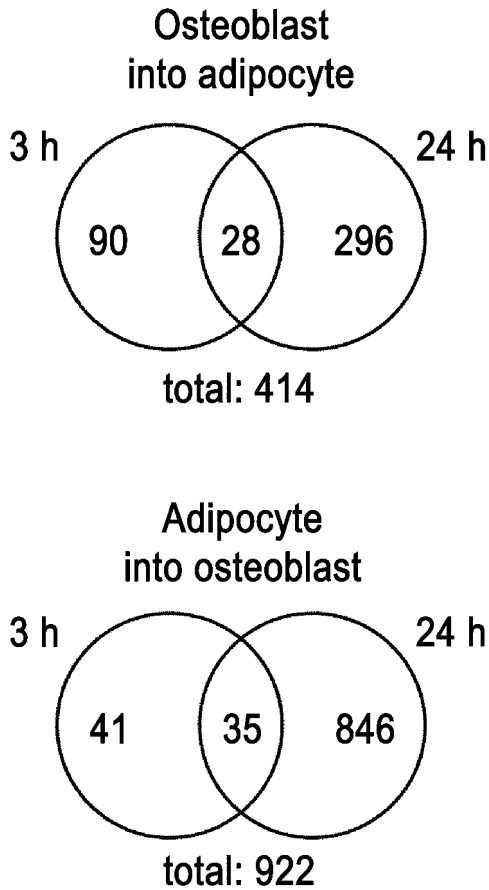

Fig. 2. Venn diagrams showing the number of reproducibly regulated genes during transdifferentiation. Included genes displayed at least twofold changes of expression during transdifferentiation compared to normally differentiated control samples. For each transdifferentiation direction, the number of genes regulated only 3 h or only 24 h after initiation of transdifferentiation is depicted in the left and the right circle, respectively. The intersection indicates the number of genes regulated at both time points examined.

patterns were in accordance for both analysis methods in 82%.

Assessment of the Relevance of Differentially Expressed Genes by Their Bioinformatic Score and Function

To sort the obtained regulated genes by relevance, we developed a novel scoring scheme that not only took into account the absolute values of fold changes but also incorporated change *P*-values, reciprocity of the regulation in the different transdifferentiation directions and also correlation between repeated experiments (see Materials and Methods' section). Employing this score provided the ranking of regulated genes. The 50 most highly ranked genes are listed in Table IV. The complete ranking can be found online (supplementary Table VI). The fold changes of the 8 highest-ranking regulated genes are depicted in Figure 4. As for many of the regulated genes, expression of these 8 genes showed a reciprocal regulation pattern between the different transdifferentiation events at least at one of the two time points examined. Among the 50 most highly ranked genes, many differentially expressed genes are associated with distinct signaling pathways, morphology, cell differentiation, lipid metabolism, cellular biosynthesis, and transcription. Furthermore, 31 of the top 50-ranking genes were members of over-represented GO classes as detected by GOstat analysis (Table II and supplementary Table V).

Taking all reproducibly and at least twofold regulated genes into account revealed regulation in various signaling pathways such as FGF signaling, insulin-like growth factor (IGF) signaling, integrin signaling, Wnt/β-catenin signaling, G-protein signaling, and plasminogen activator urokinase (PLAU) signaling (Table V). Additionally, some genes associated with lipid metabolism, adenosine triphosphate (ATP) metabolism, and adipogenesis were found.

Influence of FGF1 on Adipogenic Lineage Development

FGF1 as one of the potential key factors involved in transdifferentiation clearly inhibited adipogenic differentiation. The formation of lipid vesicles was abolished or strongly reduced in comparison to control samples incubated in adipogenic medium without FGF1 (Fig. 5). Thereby after 7 days of incubation, concentrations of 6–25 ng/ml FGF1 (Fig. 5F,H,J) had a strong inhibitory effect, whereas single lipid vesicles were detected after 14 days of incubation (Fig. 5G,I,K), especially for the lowest concentration (6 ng/ml) of FGF1 (Fig. 5G). Semiquantitative determination of lipid vesicle-containing areas showed a significant inhibition of adipogenic differentiation for all FGF1 concentrations applied when compared to the adipogenic control (Fig. 6). The application of heparin commonly used to support the function of FGF1 [Wesche et al., 2005] had no significant influence on adipogenic differentiation when applied alone (Figs. 5D,E and 6).

TABLE II. Major Over-Represented GO Classes

GO ID	GO term	Gene symbol	Regulated genes (all)	GOstat *P*-value
		3 h after initiation of adipogenic transdifferentiation		
		Biological process		
GO:0007275	Development	**EPHA2** APOLD1 SLC2A14 SIX2 ENC1 EGR2 **KLF6** CXCL1 LIF DLX5 HMGA2 HLX1 KLF4 SEMA4C **CYR61** EGR3 BICD1 TGIF	18 (736)	0.000858
GO:0006350	Transcription	**NR4A2** SIX2 KLF7 CBX4 CREM ZNF281 **ID4** EGR2 **KLF6** ZNF331 HIVEP1 CHD1 DLX5 KLF4 HLX1 HMGA2 ZNF217 EGR3 TCF8 TGIF MSC	21 (1064)	0.0025
GO:0007165	Signal transduction	EPHB3 **EPHA2** CCL20 STK38L TNFRSF1B DUSP6 **RASD1 NR4A2** CREM GPR157 RGS2 **RAB20** GPRC5A PTGER4 CXCL1 LIF GNAL ITGAV CCL3	19 (1117)	0.0342
		Molecular function		
GO:0030528	Transcription regulator activity	**NR4A2** KLF7 SIX2 CBX4 CREM ZNF281 **ID4** EGR2 **KLF6** DLX5 HLX1 KLF4 EGR3 ZNF217 TCF8 TGIF MSC	17 (588)	0.0000595
GO:0004871	Signal transducer activity	RGS2 GPRC5A PTGER4 EPHB3 **EPHA2** CCL20 CXCL1 LIF TNFRSF1B GNAL SEMA4C **NR4A2** ITGAV CCL3 GPR157	15 (773)	0.0339
		24 h after initiation of adipogenic transdifferentiation		
		Cellular component		
GO:0005576	Extracellular region	UACA CHL1 CSPG4 IL32 LPL **IGF1** ANGPTL2 ECGF1 **TNFRSF11B** CX3CL1 MMP1 FGF2 CXCL13 WNT5B FGF1 CXCL12 COL13A1 LEP **CYR61** IGFBP5 PRL **SERPINE1** PLA2G5 FN1	24 (353)	0.000014
GO:0005856	Cytoskeleton	FBLIM1 DIAPH1 UACA **TPM1** STK38L RAPH1 VASP FGD4 FSCN1 CFL2 CALD1 RP11-54H7.1 ACTG2 NEDD9 MICAL2 PDLIM7 PLEKHC1 ACTC CTNNAL1 MYLIP DSP TUBB6 SMTN PALLD	24 (363)	0.0000154
		Biological process		
GO:0007275	Development	HOP CHL1 EBF DDIT4L BDNF FZD4 CYP1B1 CHGN DSCR1L1 **PDLIM5** HDAC9 GLDN CLTCL1 FABP5 FGF1 PDLIM7 HMGA2 TNFRSF12A **CYR61** SORT1 **PPARGC1A** AHNAK PRL DSP CEBPA FBLIM1 CSPG4 EYA1 **IGF1** ANGPTL2 FGD4 ROR2 CAP2 VEGFC PALMD **TNFRSF11B** ECGF1 BHLHB3 FGF2 MAFB ARNT2 WNT5B NEDD9 **KLF6** PLEKHC1 IGFBP5 MYLIP MKX SMTN	49 (771)	4.99×10^{-11}
GO:0007165	Signal transduction	CHL1 LRRFIP2 CMKOR1 FZD4 ARHGAP28 **SNF1LK2** ARHGAP29 INPP4B ARL4C DSCR1L1 CX3CL1 **RGS4 RAB20** FGF1 **ANKRD1** SGK3 **PPARGC1A** PRL SERPINB9 CEBPA **PLCB4** DIRAS3 FN1 SPHK1 CSPG4 CD97 STK38L RAPH1 PDE7B **IGF1** FGD4 ROR2 TNS3 **RASD1** CAP2 VEGFC CLIC3 **TNFRSF11B** ECGF1 ADCY7 FGF2 ARNT2 WNT5B TAS2R38 NEDD9 GPR176 RAB3B HMOX1 OXTR CXCL12 GNAL LEP IGFBP5	53 (1170)	0.0000202
		Molecular function		
GO:0004871	Signal transducer activity	DIAPH1 MICB CMKOR1 LOXL4 BDNF LRP4 FZD4 **PDLIM5** CX3CL1 **RGS4** CLTCL1 FGF1 TNFRSF12A **PPARGC1A** SORT1 PRL **PLCB4** CD97 EVI2A CSPG4 IL32 **IGF1** ANGPTL2 ROR2 GMFG VEGFC ECGF1 **TNFRSF11B** FGF2 CXCL13 WNT5B ARNT2 TAS2R38 GPR176 HMOX1 OXTR CXCL12 GNAL LEP	39 (794)	0.000196
GO:0008092	Cytoskeletal protein binding	DIAPH1 **TPM1 SYNPO2** STK38L VASP FGD4 FSCN1 GMFG MYLIP CFL2 **CNN1** SMTN **PDLIM5** PALLD CALD1	15 (177)	0.00208
		3 h after initiation of osteogenic transdifferentiation		
		Cellular component		
GO:0005576	Extracellular region	MMP3 GDF15 MMP12 **ANGPTL4** COL1A2	5 (344)	0.0782
		Biological process		
GO:0044262	Cellular carbohydrate metabolism	MMP3 MMP12 **PDK4** EXT1 PCK1	5 (190)	0.0916
		Molecular function		
GO:0004871	Signal transducer activity	EDG2 ACVR1C GDF15 PBEF1 **PDLIM5 RGS4** FZD4	7 (790)	0.0938
		24 h after initiation of osteogenic transdifferentiation		
		Cellular component		
GO:0005856	Cytoskeleton	DIAPH1 KIF20A ESPL1 KIF21A TPM4 TUBA1 MPHOSPH1 HIP1 BUB1 VASP AURKA MICAL1 ARPC5 MICAL2 LASP1 PPL CTNNAL1 HSPB1 KIF14 DSP CENPE PALLD PDLIM2 UACA FBLIM1 RAI14 BUB1B **TPM1** LMNB1 KIF11 RAPH1 CKAP2 SPAG5 FSCN1 DBN1 EPB41L2 CALD1 ACTG2 KIF4A LOC146909 TTK NEDD9 RACGAP1 CDC42EP5 CDC20 TPX2 KNS2 KIF23 WDR1 MYLIP NEK2 ANLN EPB41L3 PRC1 SGCD KIF15 SMTN TPM2 KIF2C DLG7 ARHGDIB	61 (379)	2.84×10^{-11}

GO:0005576	Extracellular region	MMP13 CHL1 MMP12 **IGFBP1** APOL6 PLAT GLIPR1 YARS GREM2 FSTL3 MFAP5 PRRG4 PDGFA FGF1 SAA2 **CYR61** LAMA4 VEGF CHI3L1 **SERPINE1** COMP CLEC3B COL11A1 FN1 UACA THBS1 ANGPTL2 HAPLN1 PHGDH **TNFRSF11B** CXCL13 WNT5B GDF15 CXCL12 **ANGPTL4** WISP1 LEP COL8A1 SGCD CTGF ADIPOQ	41 (362)	0.00397
GO:0005694	Chromosome	BUB1B RFC3 MAD2L1 BUB1 TMPO HNRPD MCM2 CDCA5 AURKB ZWILCH RAD50 CBX5 TOP2A PRRX2 SGOL2 HMGA2 KNTC2 MCM7 CHEK1 CENPE CDCA8 KIF2C	22 (159)	0.00628
		Biological process		
GO:0007049	Cell cycle	CDKN3 ESPL1 DDIT3 BUB1 E2F7 AURKB RAD50 PBK E2F8 PDGFA FGF1 MCM5 CDC6 RGC32 MCM6 CHEK1 DIRAS3 HRASLS3 KIF11 MKI67 CKAP2 CEP55 MCM2 BARD1 CDK6 CCND3 YWHAH RACGAP1 CDC20 BRIP1 TPX2 PTTG1 NEK2 ANLN KIF15 KIF2C DLG7 UHRF1 HK2 ZWINT CDCA5 PLK1 CCNB1 AURKA TCF19 CDC2 HDAC9 NUSAP1 SGOL2 MSH2 UBE2C WEE1 VEGF CIT CENPE BUB1B MAD2L1 BRRN1 SPAG5 SPIN3 CCND1 PLK4 VEGFC CCNA2 CCNB2 NEDD9 TTK CCNE2 KIF23 KNTC2 MCM7 PRC1 SESN2 CDCA8 HCAP-G	75 (462)	1.13×10^{-14}
GO:0007010	Cytoskeleton organization and biogenesis	DIAPH1 KIF20A ESPL1 KIF21A TUBA1 ZWINT MPHOSPH1 AURKA ADRA2A MICAL1 ARPC5 NUSAP1 LASP1 UBE2C KIF14 **CNN1** CENPE PALLD BUB1B KIF11 FSCN1 SPAG5 DBN1 EPB41L2 LOC146909 KIF4A YWHAH CDC42EP5 RACGAP1 NEDD9 TTK KNS2 KIF23 CXCL12 KNTC2 PRC1 EPB41L3 SGCD KIF15 KIF2C ARHGDIB	41 (201)	1.45×10^{-11}
GO:0007275	Development	EMP1 EBF **IGFBP1** CASC5 FOXC2 BDNF NRCAM SLC3A2 SEMA6D CSRP2 EDNRB NTRK2 TAGLN FGF1 PPL TNFRSF12A LAMA4 **CYR61** **PPARGC1A** IFRD1 CLEC3B COL11A1 **EPHA2** PALMD CAP2 DBN1 PHGDH SOX9 **TNFRSF11B** MEOX2 IER3 WNT5B YWHAH LPIN1 RACGAP1 HLF WISP1 MYLIP CTGF CAP1 CHL1 DDIT4L ALDH3A2 GPM6B NRAS FZD4 CYP1B1 TAGLN2 ALPL SEMA3G GHR DLX1 **PDLIM5** CACNB2 PRRX2 HDAC9 TGFBR3 DACT1 HMGA2 FHL3 VEGF CIT DSP MET COMP EFNB2 FBLIM1 THBS1 ANGPTL2 CEBPG SEMA5A SPIN3 VEGFC VLDLR BHLHB3 ARNT2 NEDD9 CDC42EP5 **KLF6** MBNL1 **ANGPTL4** SGCD SMTN KITLG ARHGDIB	85 (786)	0.0000117
GO:0007165	Signal transduction	CLOCK **IGFBP1** KIT CMKOR1 GKAP1 ITGA3 ARHGAP28 SCG5 AGTR1 INPP4B OPN1SW ARL4C EDNRB PXK ITGA5 **RAB20** NTRK2 PLEKHG2 **DDAH1** PDGFA FGF1 **ANKRD1** **PPARGC1A** BAG1 **PLCB4** ILK DIRAS3 CLIC1 **EPHA2** ARHGAP22 **RASD1** IL4R CAP2 FAM13A1 ADCY7 **TNFRSF11B** PRKAR2B RAC2 YWHAH WNT5B TAS2R38 GDF15 RACGAP1 PPP4R1 HMOX1 CXCL12 GNAL WISP1 PBEF1 RHOC CAP1 GNB4 CHL1 ZWINT PLP2 FZD4 **SNF1LK2** AURKA ADRA2A SAV1 MICAL1 TOP2A SLC20A1 MKNK2 **RGS4** FEN1 PTGFR TGFBR3 DACT1 IL18R1 LIFR UBE2C VEGF CIT GEM MET ZYX FN1 BUB1B CD97 RAPH1 PDE7B SPAG5 VEGFC VLDLR TXNRD1 PDE3B RAGE ARNT2 TNFRSF21 NEDD9 ECT2 ARHGEF2 RAB3B FPR1 DEPDC1 ARHGAP18 LEP KNTC2 DAPK3 TGFB1I1 PTGER2 RASL11B KITLG ARHGDIB	105 (1228)	0.0106
		Molecular function		
GO:0008092	Cytoskeletal protein binding	DIAPH1 **TPM1** TPM4 HIP1 VASP FSCN1 NRCAM DBN1 PXK **PDLIM5** EPB41L2 CALD1 YWHAH RACGAP1 TAGLN LASP1 MYLIP WDR1 ANLN EPB41L3 **CNN1** TPM2 SMTN CAP1 PALLD	25 (182)	0.021
GO:0000166	Nucleotide binding	RFC3 KIF21A REV3L TUBA1 KIT BUB1 DHRS3 AURKB SCG5 PBK RAD50 ARL4C FIGNL1 **RAB20** NTRK2 MCM5 ACACB CDC6 RP11-301I17.1 PC **PPARGC1A** MCM6 CHEK1 TK1 MELK CIRBP MXRA5 ILK DIRAS3 KIF11 ATAD2 **PDK4** **EPHA2** GBP1 MKI67 HNRPD MCM2 **RASD1** PRKAR2B RAC2 LOC91461 TRIP13 MCM4 ACTG2 LOC146909 CDK6 FAM83D TPX2 BRIP1 GNAL NEK2 KIF15 RHOC KIF2C KIF20A PCK2 DOCK11 TRIB3 HK2 POR MPHOSPH1 PLK1 DCK LOC81691 **SNF1LK2** AURKA CDC2 YARS TOP2A MKNK2 MSH2 WEE1 EHD1 KIF14 CIT GEM MET CENPE BUB1B RP2 PLK4 RRM1 LARP6 TXNRD1 SPG3A ME1 RAGE KIF4A TTK THNSL1 RAB3B FRY KIF23 MCM7 DAPK3 RASL11B	96 (113)	0.0516
GO:0004871	Signal transducer activity	CLOCK KIT CMKOR1 ITGA3 BDNF SEMA6D OPN1SW AGTR1 EDNRB GREM2 ITGA5 NTRK2 PDGFA **FGF1** LASP1 TNFRSF12A SAA2 LAMA4 **PPARGC1A** BAG1 **PLCB4** NR1H3 MXRA5 **EPHA2** IL4R NR1D2 **TNFRSF11B** WNT5B YWHAH GDF15 TAS2R38 HMOX1 CXCL12 GNAL PBEF1 RHOC ULBP2 GNB4 DIAPH1 LOXL4 FZD4 ADRA2A GHR SEMA3G YARS **PDLIM5** SLC20A1 **RGS4** TGFBR3 PTGFR LIFR IL18R1 VEGF MET EFNB2 THBS1 EVI2A CD97 ANGPTL2 SEMA5A IGSF4 VLDLR VEGFC CXCL13 PDCD1LG2 TNFRSF21 ARNT2 ECT2 FPR1 LEP KDELR3 TGFB1I1 PTGER2 KITLG ADIPOQ	75 (834)	0.0527

Reliably measured Affymetrix probe sets (for each experimental set at least one P detection call in the compared samples) displaying differential regulation after initiation of adipogenic and osteogenic transdifferentiation were subjected to GOstat analyses. The total number of regulated and not regulated Affymetrix IDs detected on the GeneChip for each GO class served as reference and is given in parentheses behind the number of regulated genes. Only those over-represented GO classes were taken into account that comprised at least 5 genes and a GOstat $P \leq 0.1$. The table displays only a selection of the major over-represented GO classes, a complete list is available as supplementary Table V. For adipogenic transdifferentiation, the 3 h samples provided 159 differentially regulated target probe sets that were analyzed in reference to all 20,357 reliably measured probe sets at this time point, the 418 target probe sets of the 24 h samples were referred to 21,892 reliably measured probe sets on the GeneChip. For osteogenic transdifferentiation, 92 target probe sets obtained 3 h after initiation of transdifferentiation were analyzed to the reference of all 22,634 reliably measured probe sets at this time point, the 24 h samples provided 1,196 target probe sets that were analyzed to the reference of all 24,108 reliably measured probe sets on the GeneChip. No relevant over-representation was found under the stated criteria for the GO class of cellular component 3 h after initiation of adipogenic transdifferentiation. Gene names are abbreviated according to HUGO gene nomenclature. Gene symbols in bold letters indicate that the respective gene ranks amongst the top 50 of our bioinformatic scoring depicted in Table IV.

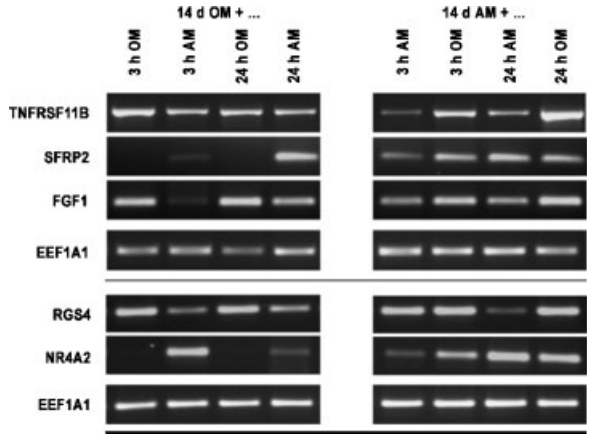

Fig. 3. Examples for re-evaluation of microarray data by semiquantitative RT-PCR. hMSCs were incubated in OM (left side) or AM (right side) for 14 days prior to initiation of transdifferentiation. Adipogenic (left side) and osteogenic reprogramming (right side) was induced by changing to the respective other differentiation medium, control samples received a fresh aliquot of the same differentiation medium as applied before. RNA samples were isolated at the indicated time points, fully differentiated adipocytes (14 days + 3 h and 14 days + 24 h in AM) and committed osteoblasts (14 days + 3 h and 14 days + 24 h in OM) served as controls. RT-PCR was performed for selected genes (Table I), eukaryotic translation elongation factor 1 alpha 1 (EEF1A1) as house keeping gene reported the quality of cDNA.

DISCUSSION

In this study, we examined transdifferentiation by employing genome-wide gene expression profiling and ranked regulated genes according to a relevance score. For each gene, this score took reproducibility, extent, and reciprocity of regulation during the adipogenic and osteogenic transdifferentiation processes into account.

Amongst those genes that displayed reproducible differential regulation during transdifferentiation at one or both time points examined, many were reciprocally regulated in the different transdifferentiation directions. The majority of genes regulated during osteogenic transdifferentiation showed elevated expression whereas declined mRNA amounts were provided for the majority of genes regulated during adipogenic transdifferentiation. This suggests that the adipogenic switch of committed osteoblasts is mainly achieved indirectly by down-regulation of gene products that would inhibit adipogenic transdifferentiation. In contrast, osteogenic transdifferentiation of adipocytes seems to require active induction of a high number of genes. Accordingly, Bäckesjö et al. [2006] delivered evidence for the importance of active repression of the adipogenic program by showing that activation of the nuclear NAD-dependent protein deacetylase sirtuin 1 diminished the adipogenic conversion of murine MSCs under osteogenic incubation conditions. Therefore, hMSCs or pre-osteoblasts that have lost the ability to repress adipogenic development could also contribute to the age- and disease-related gain of adipose tissue in bone marrow and the concomitant loss of bone mass [Meunier et al., 1971; Burkhardt et al., 1987; Koo et al., 1998; Nuttall and Gimble, 2000; Pei and Tontonoz, 2004; Gimble et al., 2006; Rosen and Bouxsein, 2006].

Examination of regulated probe sets by GOstat analyses provided over-represented groups of genes affiliated to the same cellular component, biological process or molecular function. Thereby, genes associated with signal transduction were enriched in both transdifferentiation directions and for both time points examined, whereas transcription-related genes were only over-represented 3 h after initiation of adipogenic transdifferentiation. Furthermore, the GO classes of extracellular region, morphogenesis, and cytoskeleton were mainly over-represented 24 h after initiation of transdifferentiation. This suggests that transdifferentiation involves signaling pathways and alteration of development-associated gene products. Thereby, adipogenic transdifferentiation starts with transcription-associated events 3 h after initiation of transdifferentiation, whereas morphogenesis-, cytoskeleton-, and extracellular matrix-related genes are activated in both transdifferentiation directions after 24 h. Additionally 24 h after initiation of osteogenic transdifferentiation, the accumulation of cell cycle- and chromosome-associated genes indicates a profound change of the cellular state.

Shortly after initiation of adipogenic transdifferentiation, the microarray analyses detected the up-regulation of the adipogenesis-associated genes LPL and FABP4 (PPARG2 was up-regulated below threshold with a signal log ratio of 0.7), while in the reverse osteogenic transdifferentiation of adipocytes none of the known markers for osteogenesis showed twofold or higher differential regulation. Semiquantitative RT-PCR analyses confirmed the increase of LPL expression and additionally showed enhancement of PPARG2 mRNA levels 24 h after initiation of adipogenic transdifferentiation (both less than twofold; data not

TABLE III. Accordance of Microarray Data and RT-PCR Analyses

Gene name	Fold change: RT-PCR analysis	Fold change: Microarray analysis	Transdifferentiation processes	Accordance
Cysteine-rich, angiogenic inducer, 61 (CYR61)	−2.6	−3.7 −3.8	OB into AC: 3 h	++
	−8.5	−10.9 −24.3	OB into AC: 24 h	++
	6.6	9.6 13.6	AC into OB: 24 h	++
Fatty acid binding protein 4, adipocyte (FABP4)	15.5	20.4 62.2	OB into AC: 24 h	++
Fibroblast growth factor 1 (FGF1)	−2.4	−7.3 −6.0 −9.6	OB into AC: 24 h	+
	2.2	22.3 5.0 16.2	AC into OB: 24 h	+
G0/G1switch 2 (G0S2)	30.4	19.3	OB into AC: 24 h	++
	−1.3	−3.0	AC into OB: 24 h	+
Insulin-like growth factor 1 (somatomedin C) (IGF1)	4.4	17.4 5.1 7.2 8.3	OB into AC: 24 h	++
	−3.0	−3.4 −2.6	AC into OB: 24 h	++
Kruppel-like factor 6 (KLF6)	−4.5	−2.5 −2.1	OB into AC: 3 h	++
	−1.2	−3.2 −3.1	OB into AC: 24 h	+
	−2.6	2.3 2.1	AC into OB: 3 h	−
	1.9	2.8 2.5	AC into OB: 24 h	+
Nuclear receptor subfamily 4, group A, member 2 (NR4A2)	Not detectable in control	15.8 17.8 15.2	OB into AC: 3 h	++
	Not detectable in control	7.0 6.7 5.1	OB into AC: 24 h	++
	2.5	−3.5 −5.4	AC into OB: 3 h	−
Regulator of G-protein signaling 4 (RGS4)	−2.5	−5.5 −9.4 −13.5	OB into AC: 3 h	++
	−1.7	−3.2 −5.0 −8.6	OB into AC: 24 h	+
	1.0	1.9 2.1 2.1	AC into OB: 3 h	−
	4.8	16.0 25.6 39.9	AC into OB: 24 h	++

(*Continued*)

TABLE III. (*Continued*)

Gene name	Fold change: RT-PCR analysis	Fold change: Microarray analysis	Transdifferentiation processes	Accordance
Secreted frizzled-related protein 2 (SFRP2)	Not detectable in control	18.3 10.8	OB into AC: 24 h	++
	−1.0	−22.5 −4.5	AC into OB: 24 h	−
Serpin peptidase inhibitor, clade E (nexin, plasminogen activator inhibitor type 1), member 1	−31.1	−4.0 −4.8 −3.6	OB into AC: 24 h	++
(SERPINE1)	−2.3	1.2 3.2 1.0	AC into OB: 3 h	−
	4.2	7.2 14.6 12.8	AC into OB: 24 h	++
Tumor necrosis factor receptor superfamily, member 11b	−2.2	−8.9 −19.2	OB into AC: 24 h	+
(osteoprotegerin) (TNFRSF11B)	3.4	21.6 29.4	AC into OB: 24 h	++

Fold changes obtained by RT-PCR and microarray analysis are depicted in the respective columns. Up-regulation is stated by positive values whereas negative values correspond to down-regulation. Where more than one value per gene product is given for microarray data, different probe sets for the same gene showed regulation. Accordance of RT-PCR and microarray data was assessed for identical RNA samples employing following criteria:
+, same algebraic sign and $-2.5 <$ fold change ≤ -1.2 or $1.2 \leq$fold change <2.5.
++, same algebraic sign and fold change ≤ -2.5 or fold change ≥ 2.5.
−, meeting none of the above described criteria.

shown). For osteogenic transdifferentiation, RT-PCR analyses detected less than twofold increases in ALP and BGLAP expression shortly after the initiation of osteogenic transdifferentiation (data not shown) which was in accordance with the microarray data displaying only genes with at least twofold regulation. Thus at least in part, the genes involved in the initiation of transdifferentiation seem to be different from established differentiation-specific markers. Therefore, we developed a novel empirical bioinformatic scoring scheme that provides differentially regulated genes with potentially high relevance in the processes of transdifferentiation. Thereby, the proposed scoring scheme not only included the change of expression for one transdifferentiation event but also awarded the reciprocal regulation in the different transdifferentiation directions and thus enabled the ranking of relevant gene products. The reciprocal regulation of both processes seemed very important, since it would provide an effective means to balance and regulate osteogenic and adipogenic differentiation. Furthermore, a reciprocal relationship has been reported for adipogenic and osteogenic differentiation in which factors of one differentiation pathway inhibited the other [Akune et al., 2004; Nuttall and Gimble, 2004]. The detection of more than 60% of the top 50-ranking genes as members of over-represented GO classes supported the relevance of these genes in the initiating events of transdifferentiation and thus confirmed the usefulness of our bioinformatic scoring scheme.

Interestingly, members of FGF signaling were differentially regulated in our experiments. FGF1 even displayed a reciprocal regulation pattern in the different transdifferentiation events suggesting that secreted FGF1 has an autocrine function that promotes osteogenic transdifferentiation by inhibiting adipogenic development. To demonstrate that our bioinformatic scoring system detects functionally relevant gene products, we performed an assay that proved the inhibitory effect of externally applied FGF1 on adipogenic differentiation in our cell culture system. In human pre-adipocytes, FGF1 has been reported to accelerate adipogenesis [Hutley et al., 2004]. However, this result could be a consequence of the proliferative effect of FGF1 on subconfluent

TABLE IV. Top 50 of Regulated Genes During Transdifferentiation

#	Adipogenic transdiff.	Osteogenic transdiff.	Combined score	Correlation	Score 1	Score 2	Number of probe sets	Gene symbol	Gene name	Functions
1	Down	Up	42.47	0.89	49.37	46.12	3	RGS4	Regulator of G-protein signaling 4	a, g
2	Down	Up	32.28	0.94	28.62	40.21	2	TNFRSF11B	Tumor necrosis factor receptor superfamily, member 11b	a, k
3	Down	Up	32.27	0.97	28.68	37.68	1	KRTAP1-5	Keratin associated protein 1–5	
4	Down	Up	31.07	0.79	36.14	42.40	7	SYNPO2	Synaptopodin 2	
5	Up	Down	30.93	0.82	−32.98	−42.65	5	PHLDA1	Pleckstrin homology-like domain, family A, member 1	
6	Down	Up	29.31	0.93	24.43	38.64	2	PLCB4	Phospholipase C, beta 4	a, d, g
7	Up	Down	28.64	0.95	−29.83	−30.33	2	SFRP2	Secreted frizzled-related protein 2	a, c
8	Up	Down	28.38	0.78	−34.39	−38.87	3	NR4A2	Nuclear receptor subfamily 4, group A, member 2	a, f
9	Down	Up	28.11	0.99	28.35	28.47	1	ANKRD1	Ankyrin repeat domain 1	a
10	Down	Up	28.01	0.94	28.93	30.57	1	KRTHA4	Keratin, hair, acidic, 4	
11	Up	Down	28.00	0.94	−26.32	−33.12	3	ARL7	ADP-ribosylation factor-like 7	
12	Down	Up	27.98	0.99	23.83	32.64	2	FGF1	Fibroblast growth factor 1	a, b, c, h
13	Down	Up	27.88	0.98	23.47	33.21	1	MGAM	Maltase-glucoamylase	
14	Down	Up	26.90	0.85	31.80	31.70	2	FMN2	Formin 2	a
15	Down	Up	26.28	0.89	21.54	37.29	2	CYR61	Cysteine-rich, angiogenic inducer, 61	b
16	Up	Down	25.71	0.90	−19.01	−38.01	2	ANGPTL4	Angiopoietin-like 4	b–d
17	Down	Up	25.30	0.94	21.97	31.75	4	TPM1	Tropomyosin 1	a, d, e
18	Up	Down	24.78	0.99	−24.21	−26.12	1	RASD1	RAS, dexamethasone-induced 1	a
19	Up	Down	24.25	0.88	−18.36	−36.60	1	SLC16A6	Solute carrier family 16, member 6	
20	Down	Up	23.81	0.66	51.56	20.24	2	B3GALT2	UDP-Gal:betaGlcNAc beta 1,3-galactosyltransferase, polypeptide 2	e
21	Up	Down	23.48	0.84	−33.91	−21.89	1	PDK4	Pyruvate dehydrogenase kinase, isoenzyme 4	
22	Down	Up	23.33	0.97	24.12	23.94	1	BIRC3	Baculoviral IAP repeat-containing 3	a, l
23	Down	Up	22.97	0.94	25.91	22.92	2	SERPINE1	Serpin peptidase inhibitor, clade E, member 1	m
24	Down	Up	22.96	0.93	30.39	19.27	4	VIL2	Villin 2 (ezrin)	b, j
25	Up	Down	22.72	1.00	−21.52	−24.11	1	DDIT4	DNA-damage-inducible transcript 4	
26	Up	Down	22.40	0.89	−24.26	−26.17	3	ID4	Inhibitor of DNA binding 4, dominant negative helix-loop-helix protein	f
27	Down	Up	21.90	0.93	22.33	24.65	2	ALDH1B1	Aldehyde dehydrogenase 1 family, member B1	
28	Down	Up	21.87	0.99	22.37	21.76	1	SCHIP1	Schwannomin interacting protein 1	
29	Down	Up	21.86	0.86	21.13	29.76	3	DDAH1	Dimethylarginine dimethylaminohydrolase 1	a
30	Down	Up	21.74	0.97	18.56	26.15	1	MRVI1	Murine retrovirus integration site 1 homolog	
31	Up	Down	21.08	0.79	−31.70	−21.40	4	IGF1	Insulin-like growth factor 1	a, i
32	Down	Up	20.27	0.71	30.96	26.42	4	PDLIM5	PDZ and LIM domain 5	b
33	Up	Down	19.80	1.00	−19.60	−20.02	1	FABP4	Fatty acid binding protein 4, adipocyte	o
34	Down	Up	19.75	0.99	23.27	16.84	2	DNAJB4	DnaJ homolog, subfamily B, member 4	
35	Down	Up	19.56	1.00	18.61	20.61	1	CNN1	Calponin 1, basic, smooth muscle	
36	Up	Down	19.55	0.94	−17.56	−24.17	2	PDE4B	Phosphodiesterase 4B, cAMP-specific	a, n
37	Down	Up	19.49	0.99	20.66	18.59	2	KLF6	Kruppel-like factor 6	b, c, f
38	Up	Down	19.18	0.96	−16.47	−23.38	3	INSIG1	Insulin induced gene 1	
39	Down	—	19.02	1.00	17.03	21.00	1	CCL3L1	Chemokine ligand 3-like 1	a
40	Up	Down	18.86	1.00	−18.50	−19.37	1	RAB20	RAB20, member RAS oncogene family	a
41	Up	Down	18.75	0.80	−10.55	−36.58	1	IGFBP1	Insulin-like growth factor binding protein 1	a, b, i, j
42	Down	Up	18.46	0.99	21.19	16.03	2	LOC340061	Hypothetical protein LOC340061	
43	Up	Down	18.45	0.97	−21.88	−16.28	2	SNF1LK2	SNF1-like kinase 2	a
44	Up	Down	18.26	0.99	−18.60	−18.28	1	PPARGC1A	Peroxisome proliferative activated receptor, gamma, coactivator 1, alpha	c, d, e, f

(*Continued*)

TABLE IV. (*Continued*)

#	Adipogenic transdiff.	Osteogenic transdiff.	Combined score	Correlation	Score 1	Score 2	Number of probe sets	Gene symbol	Gene name	Functions
45	Down*	Up*	18.06	0.89	17.81	22.74	1	EPHA2	EPH receptor A2	a
46	Up	Down	18.03	0.96	15.87	21.71	1	230795_at	230795_at (transcribed locus)	
47	Up	Down	17.96	1.00	−17.51	−18.56	1	G0S2	G0/G1 switch 2	
48	Down	Up	17.96	0.839	21.42	21.38	1	SERPINB2	Serpin peptidase inhibitor, clade B, member 2	m
49	Down	Up	17.84	0.957	17.58	19.69	1	LMO7	LIM domain 7	
50	Down	Up	17.82	0.993	16.81	19.08	1	PHLDA2	Pleckstrin homology-like domain, family A, member 2	

Gene products are sorted by descending combined score that assesses the total relevance of each gene resulting from the correlation of both individual scores 1 and 2 (see Materials and Methods' section). The number of probe sets contributing to the final score is stated in the respective column. The second and third column additionally display the up- or down-regulation of genes according to our microarray data in osteogenic and adipogenic transdifferentiation, respectively. Thereby, less than twofold regulations are given in parentheses, absence of a decrease or increase call is stated by —, and the asterisk indicates that this gene only showed reciprocal regulation at the 24 h time point, whereas the 3 h time point exhibits no regulation in osteogenic but up-regulation in adipogenic transdifferentiation.
a, signal transduction; b, morphology; c, cell differentiation; d, lipid metabolism; e, cellular biosynthesis; f, transcription; g, G-protein signaling; h, FGF signaling; i, IGF signaling; j, integrin signaling; k, osteoclastogenesis; l, inhibition of apoptosis; m, PLAU signaling; n, ATP metabolism; o, adipogenesis.

pre-adipocytes in vitro. Thereby, contact inhibition due to the confluent monolayer as a prerequisite for the beginning of adipogenic differentiation [Rosen et al., 2000] would be reached earlier than in controls not treated with FGF1. In our cell culture system, only confluent monolayers were subjected to (trans)differentiation experiments. Furthermore, the effect of FGF1 on fetal rat calvarial osteoblasts has been shown to depend on their maturation stage [Tang et al., 1996]. While proliferation in early osteoblasts was enhanced, maturation and mineralization in later osteoblast stages were decreased by FGF1. Addition of FGF1 to osteogenic medium in our cell culture system did not further accelerate osteogenic differentiation of the monolayers neither quantitatively nor temporally (data not shown). Nevertheless regarding the initiation of osteogenic transdifferentiation, these findings do not exclude a stimulatory osteogenic effect in MSC-derived adipocytes.

A further noteworthy signaling pathway with differentially regulated components is the IGF signaling pathway. Two of its members, insulin-like growth factor 1 (somatomedin C; IGF1) and insulin-like growth factor binding protein 1 (IGFBP1), are amongst the top 50 of our bioinformatic ranking. Increased mRNA levels of IGF1 during adipogenic transdifferentiation indicate an adipogenesis-enhancing effect of IGF signaling as reported by Schmidt et al. [1990]. Moreover, expression of IGF1 and IGFBPs in murine and human (pre)adipocytes suggests autocrine and paracrine ways of IGF1 signaling during adipogenesis in vitro [Boney et al., 1994; Wabitsch et al., 2000].

The transcription of some components of integrin signaling was also regulated during transdifferentiation, amongst them villin 2 (ezrin; VIL2) and IGFBP1 obtained high bioinformatic scores. VIL2 is a membrane-cytoskeletal linking protein [Berryman et al., 1993], that regulates cell–cell and cell–matrix adhesions [Hiscox and Jiang, 1999]. IGFBP1 binds to the $\alpha5\beta1$ integrin receptor and also affects focal adhesion kinase phosphorylation [Ricort, 2004]. Up-regulation of the majority of these genes during osteogenic transdifferentiation indicated changes in the actin cytoskeleton that is organized by integrins [Giancotti and Ruoslahti, 1999].

Several gene products involved in or affected by the Wnt/β-catenin signaling pathway were

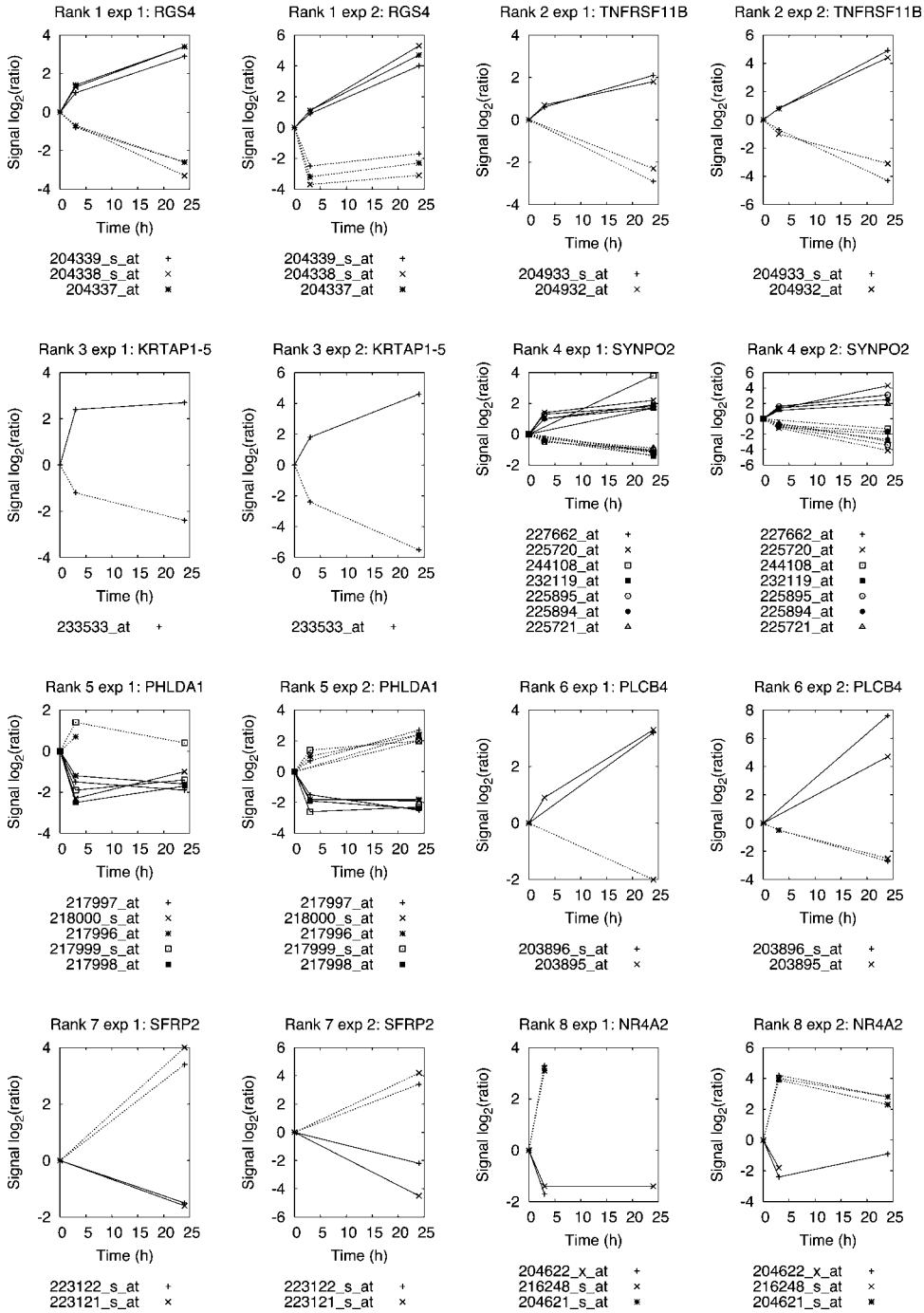

Fig. 4. Graphic illustration of gene regulation patterns of the 8 most highly ranked genes. Changes of gene expression 3 and 24 h after initiation of transdifferentiation, respectively, are given as signal $\log_2$ ratios obtained by two microarray experiments (exp. 1 and 2). Continuous curves represent transdifferentiation from adipocytes into osteoblasts, dotted curves show reprogramming of pre-osteoblasts into adipocytes. Multiple curves for the same gene in a single transdifferentiation direction represent different Affymetrix IDs for this gene. Positive signal $\log_2$ ratios indicate an increase of gene expression while negative values state a decrease of gene expression in comparison to control mRNA levels.

detected in our transdifferentiation experiments, particularly tumor necrosis factor receptor superfamily, member 11b (osteoprotegerin; TNFRSF11B), secreted frizzled-related protein 2 (SFRP2), cysteine-rich angiogenic inducer 61 (CYR61), angiopoietin-like 4 (ANGPTL4), and IGF1 were ranked amongst the 50 highest-ranking genes of our bioinformatic analysis.

TABLE V. Functional Grouping of Differentially Regulated Genes

Gene symbol	Gene name	Regulation during	
		Adipogenic transdifferentiation	Osteogenic transdifferentiation
FGF signaling			
FGF1	Fibroblast growth factor 1	Down	Up
FGF2	Fibroblast growth factor 2	Down	—
FGF7	Fibroblast growth factor 7	—	Up
BCL2	B-cell CLL/lymphoma 2	—	Down
IGF signaling			
IGF1	Insulin-like growth factor 1	Up	Down
IGFBP1	Insulin-like growth factor binding protein 1	—	Down
IGFBP5	Insulin-like growth factor binding protein 5	Up	—
PIK3R3	Phosphoinositide-3-kinase, regulatory subunit 3 (p55, gamma)	Up	—
YWHAH	Tyrosine 3-monooxygenase/tryptophan 5-monooxygenase activation protein, eta polypeptide	—	Up
CCND1	Cyclin D1	—	Up
CCND3	Cyclin D3	—	Up
PRKAR2B	Protein kinase, cAMP-dependent, regulatory, type II, beta	—	Down
Integrin signaling			
ITGA3	Integrin, alpha 3	—	Up
ITGA5	Integrin, alpha 5	—	Up
VIL2	Villin 2 (ezrin)	Down	Up
ACTG2	Actin, gamma 2, smooth muscle, enteric	Down	Up
ACTN1	Actinin, alpha 1	—	Up
ACTC	Actin, alpha, cardiac muscle	Down	—
CFL2	Cofilin 2 (muscle)	Down	Up
VCL	Vinculin	—	Up
ILK	Integrin-linked kinase	—	Up
CDC2	Cell division cycle 2, G1 to S and G2 to M	—	Up
YWHAH	Tyrosine 3-monooxygenase/tryptophan 5-monooxygenase activation protein, eta polypeptide	—	Up
IGFBP1	Insulin-like growth factor binding protein 1	—	Down
IGFBP5	Insulin-like growth factor binding protein 5	Up	—
LAMA4	Laminin, alpha 4	—	Down
Wnt/β-catenin signaling			
WNT5B	Wingless-type MMTV integration site family, member 5B	Down	Up
BIRC5	Baculoviral IAP repeat-containing 5	—	Up
FOSL1	FOS-like antigen 1	Down	—
NRCAM	Neuronal cell adhesion molecule	—	Down
CCND1	Cyclin D1	—	Up
ENC1	Ectodermal-neural cortex (with BTB-like domain)	Down	—
VEGF	Vascular endothelial growth factor	Up	Down
TLE1	Transducin-like enhancer of split 1	—	Down
TLE3	Transducin-like enhancer of split 3	Up	—
ANGPTL4*	Angiopoietin-like 4	—	Down
IGF1*	Insulin-like growth factor 1	Up	Down
SFRP2*	Secreted frizzled-related protein 2	Up	Down
CYR61*	Cysteine-rich, angiogenic inducer, 61	Down	Up
COL11A1*	Collagen, type XI, alpha 1	—	Up
CTGF*	Connective tissue growth factor	—	Up
THBS1	Thrombospondin 1	Down	Up
TNFRSF11B*	Tumor necrosis factor receptor superfamily, member 11b	Down	Up
WISP1*	WNT1 inducible signaling pathway protein 1	—	Up
G-protein signaling			
RGS4	Regulator of G-protein signaling 4	Down	Up
PLCB4	Phospholipase C, beta 4	Down	Up
GNB4	Guanine nucleotide binding protein (G protein), beta polypeptide 4	Down	Up
EDG3	Endothelial differentiation, sphingolipid G-protein-coupled receptor, 3	Up	Down
PRKAR2B	Protein kinase, cAMP-dependent, regulatory, type II, beta	—	Down
NFATC1	Nuclear factor of activated T-cells, Cytoplasmic, calcineurin-dependent 1	Up	—
NFATC4	Nuclear factor of activated T-cells, cytoplasmic, calcineurin-dependent 4	Up	—
Plasminogen activator, urokinase (PLAU) signaling			
PLAUR	Plasminogen activator urokinase receptor	—	Up
SERPINB2	Serpin peptidase inhibitor, clade B (ovalbumin), member 2	Down	—
SERPINE1	Serpin peptidase inhibitor, clade E, member 1	Down	Up
Lipid metabolism			
ACACA	Acetyl-Coenzyme A carboxylase alpha	—	Down
ACACB	Acetyl-Coenzyme A carboxylase beta	Up	Down
Adenosine triphosphate (ATP) metabolism			
PDE4B	Phosphodiesterase 4B, cAMP-specific	Up	Down
ADCY7	Adenylate cyclase 7	Down	Up
Adipogenesis-associated genes			
PPARGC1A	Peroxisome proliferative activated receptor, gamma, coactivator 1, alpha	Up	Down
FABP4	Fatty acid binding protein 4, adipocyte	Up	—
LPL	Lipoprotein lipase	Up	—
CEBPA	CCAAT/enhancer binding protein (C/EBP), alpha	Up	—

Up- and down-regulation in both transdifferentiation processes is shown for genes grouped into functional classes. The minus denotes that no expression change is detected under the defined criteria (see Materials and Methods' section), the asterisk indicates genes whose transcription is regulated by WNT3A.

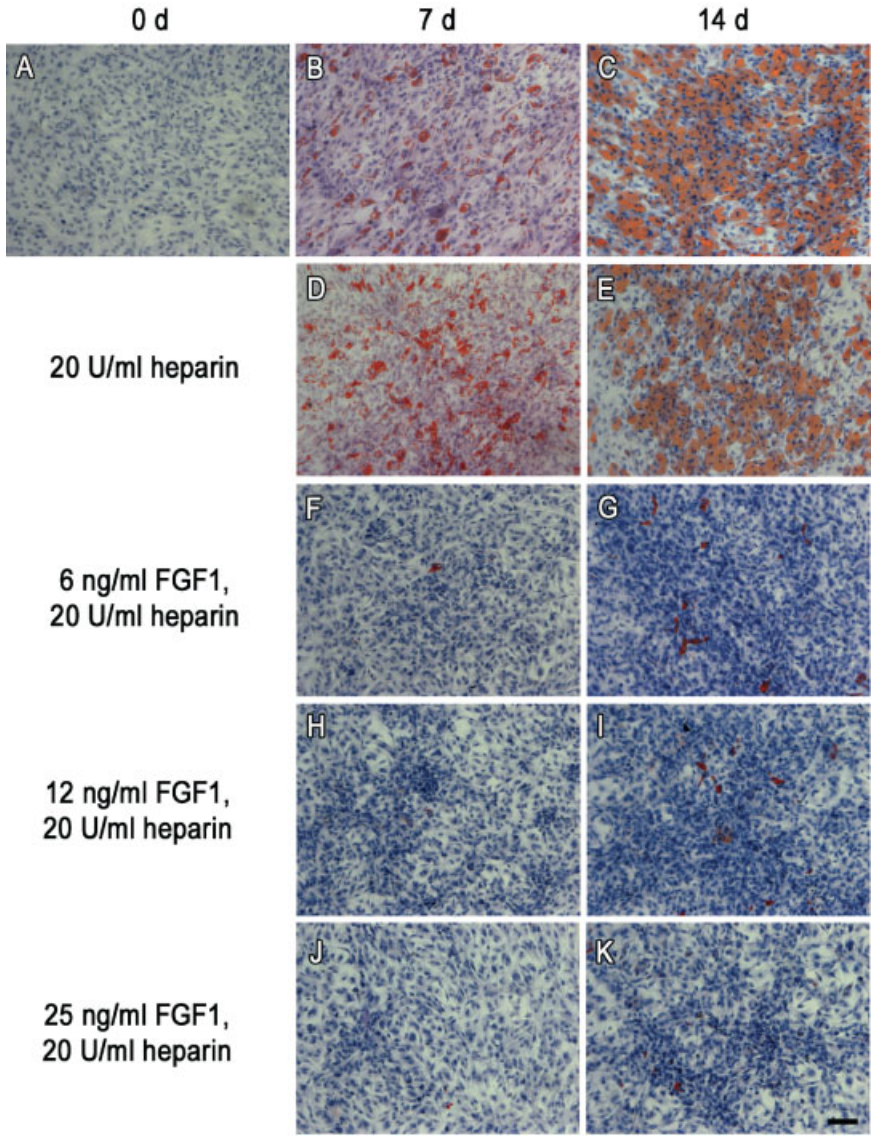

Fig. 5. Effect of FGF1 on adipogenic differentiation. Oil Red O staining of intracellular lipid vesicles and counterstaining of cell nuclei with hemalaun for normal adipogenic differentiation of hMSCs (**A**–**C**) and for incubation in AM supplemented with 20 U/ml heparin alone (**D**,**E**) or with 20 U/ml heparin plus different concentrations of FGF1 as stated on the left side (**F**–**K**). As indicated, monolayers were stained at the beginning of the experiment (0 days) and after 7 and 14 days of incubation in the respective medium. The accumulation of red lipid vesicles for incubation in AM (B,C) and in AM supplemented with heparin alone (D,E) demonstrates adipogenic differentiation. Incubation with FGF1 strongly reduced lipid vesicle accumulation (F–K). Scale bar = 100 μm.

Wnt/β-catenin signaling has been reported to promote osteogenic [Rawadi et al., 2003] and to inhibit adipogenic differentiation [Ross et al., 2000; MacDougald and Mandrup, 2002]. Interestingly, we found expression changes for genes that are regulated by wingless-type MMTV integration site family, member 3A (WNT3A) in murine C3H10T1/2 cells [Jackson et al., 2005]. Several of these genes that were differentially expressed in response to initiation of osteogenic transdifferentiation in our experiments have been shown to be similarly regulated in response to WNT3A (down-regulation of ANGPTL4, IGF1, and SFRP2 and up-regulation of CYR61, collagen, type XI, alpha 1 (COL11A1), connective tissue growth factor (CTGF), thrombospondin 1 (THBS1), TNFRSF11B, and WNT1 inducible signaling pathway protein 1 (WISP1)) [Rawadi et al., 2003]. Since WNT3A and β-catenin themselves displayed no changes of expression in our transdifferentiation experiments, their regulation

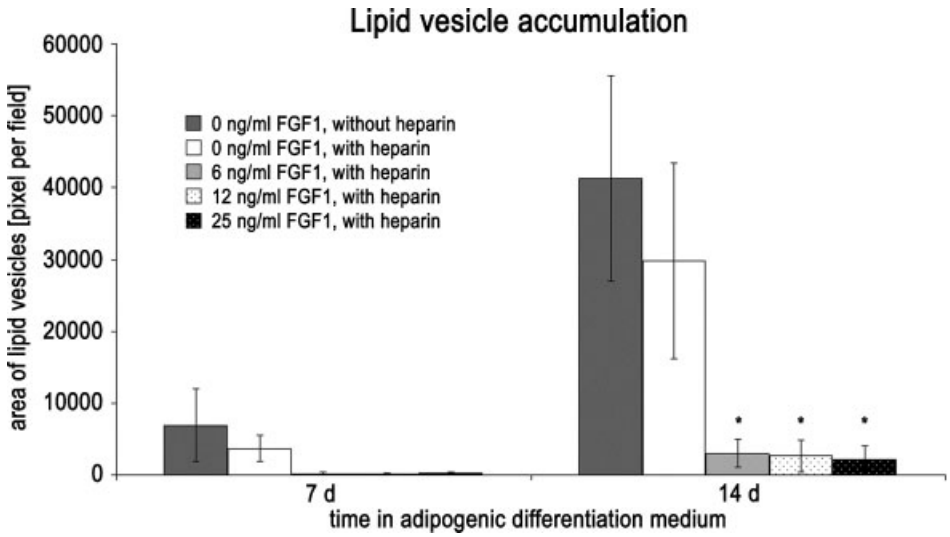

Fig. 6. Semiquantitative evaluation of lipid vesicle accumulation. Lipid vesicle-containing area after 7 and 14 days of incubation in adipogenic medium with or without heparin and FGF1 as stated. Mean ± SEM of 3 (7 days) and 4 (14 days) independent experiments with 6 fields analyzed per experiment and incubation condition. The asterisks indicate $P < 0.05$ compared to the adipogenic control (0 ng/ml FGF1, without heparin) as well as to the heparin control (0 ng/ml FGF1, with heparin).

could occur post-transcriptionally by protein–protein interactions, for example, due to the Wnt antagonist SFRP2 that has been reported to inhibit osteogenic differentiation in vitro [Oshima et al., 2005]. Additionally, Wnt signaling could act through β-catenin-independent mechanisms like the Wnt/G-protein pathway [Kohn and Moon, 2005].

Also several components of other signaling pathways or cellular processes were detected amongst the highly regulated genes during transdifferentiation. Regulator of G-protein signaling 4 (RGS4), phospholipase C, beta 4 (PLCB4), and other factors involved in G-protein signaling pointed at transmembrane signaling [Gilman, 1987]. PLAU signaling has been described to influence matrix remodeling and also integrin signaling [Choong and Nadesapillai, 2003]. Further single gene products were associated with osteoclastogenesis, lipid metabolism, and ATP metabolism. Since only few components of these processes were detected to be differentially expressed, regulation of these genes could affect new signaling pathways uniquely employed during transdifferentiation events.

The plasticity of hMSC-derived cell lineages has also been reported by others for adipocytes [Park et al., 1999] and osteoblasts [Nuttall et al., 1998; Schiller et al., 2001] even at the single cell level [Song and Tuan, 2004]. Song et al. [2006] hypothesized that transdifferentiation involves dedifferentiation prior to redifferentiation and therefore compared gene expression profiles of undifferentiated, differentiated, and dedifferentiated mesenchymal cell types. Thus, cells harvested after different periods of cultivation were compared, whereas our experimental setting related cells of the same duration of in vitro incubation. Nevertheless, regulation of some genes was detected for both studies (e.g., baculoviral IAP repeat-containing 3 (BIRC3), insulin-like growth factor binding protein 5 (IGFBP5), IGF1, laminin, alpha 4 (LAMA4), protein kinase, cAMP-dependent, regulatory, type II, beta (PRKAR2B), regulator of G-protein signaling 2 (RGS2), RGS4, serpin peptidase inhibitor, clade E, member 1 (SERPINE1), TNFRSF11B, tyrosine 3-monooxygenase/tryptophan 5-monooxygenase activation protein, eta polypeptide (YWHAH)). Therefore, some characteristics of dedifferentiation might occur in our cell culture system of transdifferentiation. However, the frequent reciprocity of gene expression changes between the different transdifferentiation directions in our cell culture system pointed at simultaneous induction of genes that are relevant to immediate transdifferentiation.

In conclusion, our study delivered insight into the genome-wide gene expression patterns shortly after the onset of adipogenic and

osteogenic transdifferentiation. Due to the known inverse relationship of the adipogenic and the osteogenic lineage, the development of a novel bioinformatic scoring scheme that outputs genes of potentially high relevance in reprogramming paid special attention to reciprocal regulation between both transdifferentiation directions. Starting from a high number of differentially regulated genes, our bioinformatic score identified potential key factors essential for initiation of transdifferentiation. FGF1 as one of these key factors has been proven to inhibit adipogenic lineage development as expected by microarray analyses and probably plays a crucial role in adipogenic transdifferentiation. Altogether, our results set the stage for further functional studies to uncover pathways and additional factors that are mandatory to initiate or inhibit the lineage switch of osteoblasts and adipocytes.

ACKNOWLEDGMENTS

We thank V.-T. Monz, M. Kunz, M. Regensburger, and J. Schneidereit for their excellent technical assistance. This study was supported by Deutsche Forschungsgemeinschaft SCHU 747/7-1 to N. Schütze and F. Jakob.

REFERENCES

Akune T, Ohba S, Kamekura S, Yamaguchi M, Chung UI, Kubota N, Terauchi Y, Harada Y, Azuma Y, Nakamura K, Kadowaki T, Kawaguchi H. 2004. PPARgamma insufficiency enhances osteogenesis through osteoblast formation from bone marrow progenitors. J Clin Invest 113:846–855.

Bäckesjö CM, Li Y, Lindgren U, Haldosen LA. 2006. Activation of sirt1 decreases adipocyte formation during osteoblast differentiation of mesenchymal stem cells. J Bone Miner Res 21:993–1002.

Barry FP, Murphy JM. 2004. Mesenchymal stem cells: Clinical applications and biological characterization. Int J Biochem Cell Biol 36:568–584.

Beissbarth T, Speed TP. 2004. GOstat: Find statistically overrepresented gene ontologies within a group of genes. Bioinformatics 20:1464–1465.

Benjamini Y, Hochberg Y. 1995. Controlling the false discovery rate: A practical and powerful approach to multiple testing. J Royal Statistical Soc B 57:289–300.

Beresford JN, Bennett JH, Devlin C, Leboy PS, Owen ME. 1992. Evidence for an inverse relationship between the differentiation of adipocytic and osteogenic cells in rat marrow stromal cell cultures. J Cell Sci 102(Pt 2):341–351.

Berryman M, Franck Z, Bretscher A. 1993. Ezrin is concentrated in the apical microvilli of a wide variety of epithelial cells whereas moesin is found primarily in endothelial cells. J Cell Sci 105(Pt 4):1025–1043.

Boney CM, Moats-Staats BM, Stiles AD, D'Ercole AJ. 1994. Expression of insulin-like growth factor-I (IGF-I) and IGF-binding proteins during adipogenesis. Endocrinology 135:1863–1868.

Burkhardt R, Kettner G, Bohm W, Schmidmeier M, Schlag R, Frisch B, Mallmann B, Eisenmenger W, Gilg T. 1987. Changes in trabecular bone, hematopoiesis and bone marrow vessels in aplastic anemia, primary osteoporosis, and old age: A comparative histomorphometric study. Bone 8:157–164.

Choong PF, Nadesapillai AP. 2003. Urokinase plasminogen activator system: A multifunctional role in tumor progression and metastasis. Clin Orthop Relat Res 415 (Suppl): S46–S58.

Darlington GJ, Ross SE, MacDougald OA. 1998. The role of C/EBP genes in adipocyte differentiation. J Biol Chem 273:30057–30060.

Ducy P. 2000. Cbfa1: A molecular switch in osteoblast biology. Dev Dyn 219:461–471.

Ducy P, Zhang R, Geoffroy V, Ridall AL, Karsenty G. 1997. Osf2/Cbfa1: A transcriptional activator of osteoblast differentiation. Cell 89:747–754.

Giancotti FG, Ruoslahti E. 1999. Integrin signaling. Science 285:1028–1032.

Gilman AG. 1987. G proteins: Transducers of receptor-generated signals. Ann Rev Biochem 56:615–649.

Gimble JM, Zvonic S, Floyd ZE, Kassem M, Nuttall ME. 2006. Playing with bone and fat. J Cell Biochem 98:251–266.

Gori F, Thomas T, Hicok KC, Spelsberg TC, Riggs BL. 1999. Differentiation of human marrow stromal precursor cells: Bone morphogenetic protein-2 increases OSF2/CBFA1, enhances osteoblast commitment, and inhibits late adipocyte maturation. J Bone Miner Res 14:1522–1535.

Haynesworth SE, Goshima J, Goldberg VM, Caplan AI. 1992. Characterization of cells with osteogenic potential from human marrow. Bone 13:81–88.

Hiscox S, Jiang WG. 1999. Ezrin regulates cell-cell and cell-matrix adhesion, a possible role with E-cadherin/beta-catenin. J Cell Sci 112 (Pt 18):3081–3090.

Hutley L, Shurety W, Newell F, McGeary R, Pelton N, Grant J, Herington A, Cameron D, Whitehead J, Prins J. 2004. Fibroblast growth factor 1: A key regulator of human adipogenesis. Diabetes 53:3097–3106.

Jackson A, Vayssiere B, Garcia T, Newell W, Baron R, Roman-Roman S, Rawadi G. 2005. Gene array analysis of Wnt-regulated genes in C3H10T1/2 cells. Bone 36:585–598.

Jaiswal N, Haynesworth SE, Caplan AI, Bruder SP. 1997. Osteogenic differentiation of purified, culture-expanded human mesenchymal stem cells in vitro. J Cell Biochem 64:295–312.

Jaiswal RK, Jaiswal N, Bruder SP, Mbalaviele G, Marshak DR, Pittenger MF. 2000. Adult human mesenchymal stem cell differentiation to the osteogenic or adipogenic lineage is regulated by mitogen-activated protein kinase. J Biol Chem 275:9645–9652.

Klein RF, Allard J, Avnur Z, Nikolcheva T, Rotstein D, Carlos AS, Shea M, Waters RV, Belknap JK, Peltz G, Orwoll ES. 2004. Regulation of bone mass in mice by the lipoxygenase gene Alox15. Science 303:229–232.

Kohn AD, Moon RT. 2005. Wnt and calcium signaling: Beta-catenin-independent pathways. Cell Calcium 38: 439–446.

Koo KH, Dussault R, Kaplan P, Kim R, Ahn IO, Christopher J, Song HR, Wang GJ. 1998. Age-related marrow conversion in the proximal metaphysis of the femur: Evaluation with T1-weighted MR imaging. Radiology 206:745–748.

Krane SM. 2005. Identifying genes that regulate bone remodeling as potential therapeutic targets. J Exp Med 201:841–843.

MacDougald OA, Mandrup S. 2002. Adipogenesis: Forces that tip the scales. Trends Endocrinol Metab 13:5–11.

Martin TJ, Sims NA. 2005. Osteoclast-derived activity in the coupling of bone formation to resorption. Trends Mol Med 11:76–81.

Meunier P, Aaron J, Edouard C, Vignon G. 1971. Osteoporosis and the replacement of cell populations of the marrow by adipose tissue. A quantitative study of 84 iliac bone biopsies. Clin Orthop Relat Res 80:147–154.

Muraglia A, Cancedda R, Quarto R. 2000. Clonal mesenchymal progenitors from human bone marrow differentiate in vitro according to a hierarchical model. J Cell Sci 113(Pt 7):1161–1166.

Nakashima K, de Crombrugghe B. 2003. Transcriptional mechanisms in osteoblast differentiation and bone formation. Trends Genet 19:458–466.

Nakashima K, Zhou X, Kunkel G, Zhang Z, Deng JM, Behringer RR, de Crombrugghe B. 2002. The novel zinc finger-containing transcription factor osterix is required for osteoblast differentiation and bone formation. Cell 108:17–29.

Nöth U, Osyczka AM, Tuli R, Hickok NJ, Danielson KG, Tuan RS. 2002a. Multilineage mesenchymal differentiation potential of human trabecular bone-derived cells. J Orthop Res 20:1060–1069.

Nöth U, Tuli R, Osyczka AM, Danielson KG, Tuan RS. 2002b. In vitro engineered cartilage constructs produced by press-coating biodegradable polymer with human mesenchymal stem cells. Tissue Eng 8:131–144.

Nuttall ME, Gimble JM. 2000. Is there a therapeutic opportunity to either prevent or treat osteopenic disorders by inhibiting marrow adipogenesis? Bone 27:177–184.

Nuttall ME, Gimble JM. 2004. Controlling the balance between osteoblastogenesis and adipogenesis and the consequent therapeutic implications. Curr Opin Pharmacol 4:290–294.

Nuttall ME, Patton AJ, Olivera DL, Nadeau DP, Gowen M. 1998. Human trabecular bone cells are able to express both osteoblastic and adipocytic phenotype: Implications for osteopenic disorders. J Bone Miner Res 13:371–382.

Oshima T, Abe M, Asano J, Hara T, Kitazoe K, Sekimoto E, Tanaka Y, Shibata H, Hashimoto T, Ozaki S, Kido S, Inoue D, Matsumoto T. 2005. Myeloma cells suppress bone formation by secreting a soluble Wnt inhibitor, sFRP-2. Blood 106:3160–3165.

Park SR, Oreffo RO, Triffitt JT. 1999. Interconversion potential of cloned human marrow adipocytes in vitro. Bone 24:549–554.

Pei L, Tontonoz P. 2004. Fat's loss is bone's gain. J Clin Invest 113:805–806.

Pittenger MF, Mackay AM, Beck SC, Jaiswal RK, Douglas R, Mosca JD, Moorman MA, Simonetti DW, Craig S, Marshak DR. 1999. Multilineage potential of adult human mesenchymal stem cells. Science 284:143–147.

Prockop DJ. 1997. Marrow stromal cells as stem cells for nonhematopoietic tissues. Science 276:71–74.

Rawadi G, Vayssiere B, Dunn F, Baron R, Roman-Roman S. 2003. BMP-2 controls alkaline phosphatase expression and osteoblast mineralization by a Wnt autocrine loop. J Bone Miner Res 18:1842–1853.

Ricort JM. 2004. Insulin-like growth factor binding protein (IGFBP) signalling. Growth Horm IGF Res 14:277–286.

Rosen CJ, Bouxsein ML. 2006. Mechanisms of disease: Is osteoporosis the obesity of bone? Nat Clin Pract Rheumatol 2:35–43.

Rosen ED, Walkey CJ, Puigserver P, Spiegelman BM. 2000. Transcriptional regulation of adipogenesis. Genes Dev 14:1293–1307.

Ross SE, Hemati N, Longo KA, Bennett CN, Lucas PC, Erickson RL, MacDougald OA. 2000. Inhibition of adipogenesis by Wnt signaling. Science 289:950–953.

Rozen S, Skaletsky H. 2000. Primer3 on the WWW for general users and for biologist programmers. Methods Mol Biol 132:365–386.

Sabatakos G, Sims NA, Chen J, Aoki K, Kelz MB, Amling M, Bouali Y, Mukhopadhyay K, Ford K, Nestler EJ, Baron R. 2000. Overexpression of DeltaFosB transcription factor(s) increases bone formation and inhibits adipogenesis. Nat Med 6:985–990.

Schiller PC, D'Ippolito G, Brambilla R, Roos BA, Howard GA. 2001. Inhibition of gap-junctional communication induces the trans-differentiation of osteoblasts to an adipocytic phenotype in vitro. J Biol Chem 276:14133–14138.

Schilling T, Nöth U, Klein-Hitpass L, Jakob F, Schütze N. 2007. Plasticity in adipogenesis and osteogenesis of human mesenchymal stem cells. Mol Cell Endocrinol, doi 10.1016/j.mce.2007.03.004.

Schmidt W, Poll-Jordan G, Loffler G. 1990. Adipose conversion of 3T3-L1 cells in a serum-free culture system depends on epidermal growth factor, insulin-like growth factor I, corticosterone, and cyclic AMP. J Biol Chem 265:15489–15495.

Schütze N, Kunzi-Rapp K, Wagemanns R, Nöth U, Jatzke S, Jakob F. 2005a. Expression, purification, and functional testing of recombinant CYR61/C CN1. Protein Expr Purif 42:219–225.

Schütze N, Nöth U, Schneidereit J, Hendrich C, Jakob F. 2005b. Differential expression of CCN-family members in primary human bone marrow-derived mesenchymal stem cells during osteogenic, chondrogenic and adipogenic differentiation. Cell Commun Signal 3:5–16.

Song L, Tuan RS. 2004. Transdifferentiation potential of human mesenchymal stem cells derived from bone marrow. FASEB J 18:980–982.

Song L, Webb NE, Song Y, Tuan RS. 2006. Identification and functional analysis of candidate genes regulating mesenchymal stem cell self-renewal and multipotency. Stem Cells 24:1707–1718.

Spiegelman BM, Choy L, Hotamisligil GS, Graves RA, Tontonoz P. 1993. Regulation of adipocyte gene expression in differentiation and syndromes of obesity/diabetes. J Biol Chem 268:6823–6826.

Tanaka T, Yoshida N, Kishimoto T, Akira S. 1997. Defective adipocyte differentiation in mice lacking the C/EBPbeta and/or C/EBPdelta gene. EMBO J 16:7432–7443.

Tang KT, Capparelli C, Stein JL, Stein GS, Lian JB, Huber AC, Braverman LE, DeVito WJ. 1996. Acidic fibroblast growth factor inhibits osteoblast differentiation in vitro: Altered expression of collagenase, cell growth-related, and mineralization-associated genes. J Cell Biochem 61: 152–166.

Verfaillie CM. 2002. Adult stem cells: Assessing the case for pluripotency. Trends Cell Biol 12:502–508.

Wabitsch M, Heinze E, Debatin KM, Blum WF. 2000. IGF-I- and IGFBP-3-expression in cultured human preadipocytes and adipocytes. Horm Metab Res 32:555–559.

Wesche J, Malecki J, Wiedlocha A, Ehsani M, Marcinkowska E, Nilsen T, Olsnes S. 2005. Two nuclear localization signals required for transport from the cytosol to the nucleus of externally added FGF-1 translocated into cells. Biochemistry 44:6071–6080.

Wu Z, Rosen ED, Brun R, Hauser S, Adelmant G, Troy AE, McKeon C, Darlington GJ, Spiegelman BM. 1999. Cross-regulation of C/EBP alpha and PPAR gamma controls the transcriptional pathway of adipogenesis and insulin sensitivity. Mol Cell 3:151–158.

Xiao G, Jiang D, Gopalakrishnan R, Franceschi RT. 2002. Fibroblast growth factor 2 induction of the osteocalcin gene requires MAPK activity and phosphorylation of the osteoblast transcription factor, Cbfa1/Runx2. J Biol Chem 277:36181–36187.